Geothermics 120 (2024) 103011

Contents lists available at ScienceDirect

Geothermics

journal homepage: www.elsevier.com/locate/geothermics

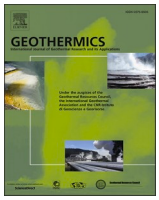

Flow-controlled thermal response test and its comparison with the conventional test methods

Murat Aydin [a,*], Ayse Ozdogan Dolcek [b], Mustafa Onur [c], Altug Sisman [d]

[a] Ruhr University Bochum, Engineering Geology and Rock Mass Mechanics, Bochum, Germany
[b] Balıkesir University, Geological Engineering, Balıkesir, Türkiye
[c] The University of Tulsa, McDougall School of Petroleum Engineering, Tulsa, OK 74104, USA
[d] Uppsala University, Department Physics & Astronomy, Uppsala, Sweden

ARTICLE INFO

Keywords:
Thermal response test
Borehole heat transfer
Ground source heat pumps
Flow-controlled thermal test

ABSTRACT

A novel flow-controlled (FC) thermal response test (TRT) system is introduced to resolve the recently addressed inconsistency between the constant heat flux (CHF) and constant temperature (CT) TRTs. FC-TRT allows us to keep both inlet and outlet temperatures constant and improve the accuracy of CT-TRT. Using the FC-TRT system, four types of TRT experiments are performed, providing CT, CHF, and constant inlet temperature conditions, besides the novel one keeping both temperature and heat flux constant. Thermal conductivities from these TRT measurements are compared, and a good agreement is observed. FC-TRT offers higher accuracy and various TRT applications in one platform.

1. Introduction

The recent energy crisis and the carbon neutral targets of the industry and governments have renewed interest in alternative energy sources such as wind, solar, geothermal, etc. In the last decade, natural gas-based systems have been widely used, especially in the European Union (EU), because of the low cost and easiness of building these systems (EU, 2021). However, the natural gas for these systems is supplied from non-EU countries, and the gas prices have increased a few times than in previous years (EU, 2021). Therefore, alternative heating and cooling systems are urgently needed for buildings. Ground source, or geothermal, heat pump systems are excellent alternatives to replace fossil-based systems (Welsch et al., 2018). Ground source heat pump (GSHP) systems extract the necessary heat energy from underground by the drilled boreholes called ground heat exchangers (GHE). They offer low operating costs and can also be used to store thermal energy to improve energy efficiency and further decrease operational costs (Guo et al., 2020). As the number of drilled boreholes increases, the drilling cost per borehole decreases and becomes more affordable for end-users. These systems are already a question of research for a long time. Some systems are monitored continuously, and it is possible to see the long-term efficiency of these systems. Specific annexes of the IEA have been exclusively dedicated to exploring this topic (Spitler and Gehlin, 2019).

Despite the high energy efficiency and low operational cost promises of GSHP systems, they can fail to reach their targeted efficiency and cost levels in the case of poor planning. As the heat is extracted from the underground, measurements of the thermal properties of the ground are crucial for the correct engineering design and planning. For a GSHP system with vertical GHE, measurements of volumetric flow rate and inlet and outlet temperatures of fluid circulating in a borehole allow the estimation of the averaged thermal properties of the ground. These measurements, called Thermal Response Test (TRT), can be performed under various conditions. The idea of TRT was first mentioned by Mogensen (1983) in a closer way to today's tests. In a typical test, a predefined constant heat power is injected into a borehole for a period using a circulation pump and a heater at the surface. It is called constant heat flux TRT (CHF-TRT). Ingersoll et al. (1954) proposed to fit the measured temperature values to the predictions of the analytical solutions of the infinite line source (ILS) approach to determine the thermal properties of the ground. Similarly, the infinite cylindrical source by Carslaw & Jeager (1959) and the finite line source by Zeng et al. (2003) approaches can also be used for CHF-TRT. In the following years, after Mogensen, some test devices were developed and used to determine the thermal properties of the ground. Besides the conventional CHF-TRT, some other TRT methods have been developed by different

* Corresponding author.
E-mail address: murat.aydin@rub.de (M. Aydin).

https://doi.org/10.1016/j.geothermics.2024.103011
Received 5 November 2023; Received in revised form 20 March 2024; Accepted 29 March 2024
Available online 3 April 2024

researchers; constant inlet temperature TRT (CIT-TRT) by Wang et al. (2010) and Aydin et al. (2014), enhanced geothermal TRT by Bussmann et al. (2016), and low power TRT by Raymond et al. (2015).

In these TRT methods, one of the control variables is kept constant while the others change throughout the experiment. In CHF-TRT, the heat rate is constant, while the circulated fluid temperature freely changes for a chosen mass flow rate (Witte, H., 2016). Beier et al. (2018) developed a multi-rate test in which the volumetric flow rate of the circulating fluid is changed intentionally, and the responses of the borehole heat exchanger (BHE) for different flow rates are obtained. Similarly, the inlet temperature is kept constant in CIT-TRT, but the heat transfer rate changes for a given flow rate. The outlet fluid temperature approaches the inlet temperature after a short while during the test, and by choosing the higher flow rates, the deviation of inlet and outlet fluid temperatures from their averaged value becomes negligible compared to the difference between average fluid and undisturbed ground temperatures. Therefore, the axial temperature is assumed to be constant and equal to the average fluid temperature during CIT-TRT. It is worth noting that the constant temperature TRTs are attractive over constant heat flux TRTs because of their advantages like having the suitability with standard heat pump tests, allowing predicting the non-stop working performance of a heat pump, and providing results closer to real working conditions of ground source heat pumps.

The developments of TRT methods are also driven by the progress in the analytical approaches. Carslaw and Jaeger (1959) used the Laplace transformation to obtain the analytical solution for the time-dependent temperature field outside a hollow cylinder for various boundary conditions. This approach has been used further to improve CIT-TRT (Aydin et al., 2019). The method was applied to CIT-TRT for various temperatures. Beier (2021) also applied this method to test the results of Choi et al. (2018). Experimental data were used to estimate the thermal conductivity of the ground, and some discrepancies from the conventional CHF-TRT results were reported.

The constant temperature assumption allows analytical solutions that agree with the exact numerical solutions only after the thermal capacity effect of BHE itself disappears (Aydin et al., 2019), like in CHF-TRT. The results are sensitive to the quality of constant-temperature conditions. Therefore, satisfying the constant-temperature condition is essential in the CIT-TRT experiment. Heaters control the inlet temperature; however, the outlet temperature is free to change, although it approaches the inlet temperature after a while. The deviation of outlet temperature from the inlet one can also be controlled by flow rate. With high flow rates, inlet and outlet temperatures become very close even at the beginning of the experiment, and the axial average fluid temperature profile is flatter than the low flow rates. Therefore, working with low flow rates causes discrepancies in determining the thermal properties. One of the solutions to keep the inlet and outlet temperatures constant and close to each other is to dynamically control the flow rates by monitoring the outlet temperature.

In this study, a flow controller is included in a TRT system to control the flow rate during the tests. In such a flow-controlled TRT (FC-TRT) system, not only the inlet temperature but also the outlet temperature is kept constant by changing the flow rate accordingly. It is called constant temperature TRT here, CT-TRT, to distinguish it from CIT-TRT. FC-TRT system also allows the CHF-TRT measurements. Using this FC-TRT unit, thermal conductivities of the ground are estimated by CIT-TRT, CT-TRT, and CHF-TRT in the same borehole and compared to each other. It is shown that there is no significant difference between the values of the thermal conductivities estimated by CHF-TRT and CIT-TRT as long as the flow rate is chosen appropriately. Therefore, the discrepancies mentioned by Beier (2021) are also resolved. Furthermore, using the flow controller, a novel TRT is realized by keeping the inlet temperature and heat flux constant, CIT&CHF-TRT, and its estimation is also discussed.

2. Method

In Fig. 1, a BHE with a single U-tube is illustrated. Here, T_{in} and T_{out} are inlet and outlet fluid temperatures, respectively. The average fluid temperature is $\overline{T}_{wf} = (T_{in} + T_{out})/2$, and r_e is the equivalent radius defined in the literature (Spitler and Bernier, 2016).

For constant borehole surface temperature, the inverse of the radial heat transfer rate per depth of a borehole is given by the following function (Aydin et al., 2019):

$$\frac{1}{q'(t)} = \beta\left[\ln(t) + \ln\left(\frac{4\alpha}{e^{\gamma}(r_e)^2}\right)\right], \tag{1}$$

where $\beta = 1/[4\pi k(\overline{T}_{wf} - T_{\infty})]$ is the slope of Eq.(1) in logarithmic time scale, k is the effective thermal conductivity of underground, W/(m·K), T_{∞} is the undisturbed underground temperature (°C), t is the time (s), α is the thermal diffusivity (m^2/s), r_e is the equivalent radius of pipes (m), and $\gamma = 0.5772$ is Euler's constant. Once the slope, β(m/W), and constant temperature difference, $\Delta T = \overline{T}_{wf} - T_{\infty}$, are known from the experimental data, the thermal conductivity is estimated from

$$k = \frac{1}{4\pi\beta\Delta T}. \tag{2}$$

On the other hand, during a CIT-TRT, although T_{in} is kept constant, T_{out} smoothly changes and approaches T_{in} depending on the volumetric flow rate $\dot{V}_f$ (m^3/h) and the borehole's thermal and geometric (especially the depth) properties. Therefore, $\overline{T}_{wf}$ and ΔT are not perfectly constant as they slightly change during the test.

Although this is a small change, it is a deviation from the constant temperature assumption of Eq. (1), and such a deviation may cause some inaccuracies in the estimation of thermal conductivity. On the other hand, the radial heat transfer rate per depth is also equal to

$$q' = \rho_f c_f \dot{V}_f (T_{in} - T_{out})/H, \tag{3}$$

where ρ_f (kg/m^3) and c_f (J/kg·K) are density and specific heat capacity of fluid, respectively, H (m) is the depth of the borehole, and $\dot{V}_f$ is the volumetric flow rate. Thus, besides keeping the inlet temperature, T_{in}, constant during the experiment, it is also possible to keep the outlet temperature, T_{out}, constant by controlling the flow rate. By setting high flow rates for the experiment, we also force the temperature difference to be small. So, to increase the accuracy of CIT-TRT, we need to keep both T_{in} and T_{out} constant and $|T_{in} - T_{out}| << |\overline{T}_{wf} - T_{\infty}|$. For this purpose, we included a flow controller in the experimental setup. Using different control algorithms for the flow controller makes it possible to perform many different TRTs, including the novel one introduced in this study, under both constant temperature and constant heat flux conditions.

A mobile TRT device used in this study is illustrated in Fig. 2. It consists of mainly a water tank, two external pipelines (for in and outflows), a circulation pump connected to the return line, 4 × 3 kW electrical resistive heaters, control valves, and measuring elements (flowmeter, temperature sensors, etc.) and the fitting elements (valves, collectors, filter, purge-air, expansion vessel, etc.).

The flow charts for two (proportional–integral–derivative) PID controllers are shown in Fig. 3. One PID reads T_{in} and controls the switches of electrical heaters, while the other PID reads T_{out} and controls the proportional valve to adjust the flow rate.

The properties of the borehole and ground are given in Table 1. The cross-section of the borehole is seen in Fig. 1. The "shank space" refers to the center-to-center distance between the inlet and outlet pipes. U-pipe spacers were utilized to keep this shank space constant along the borehole.

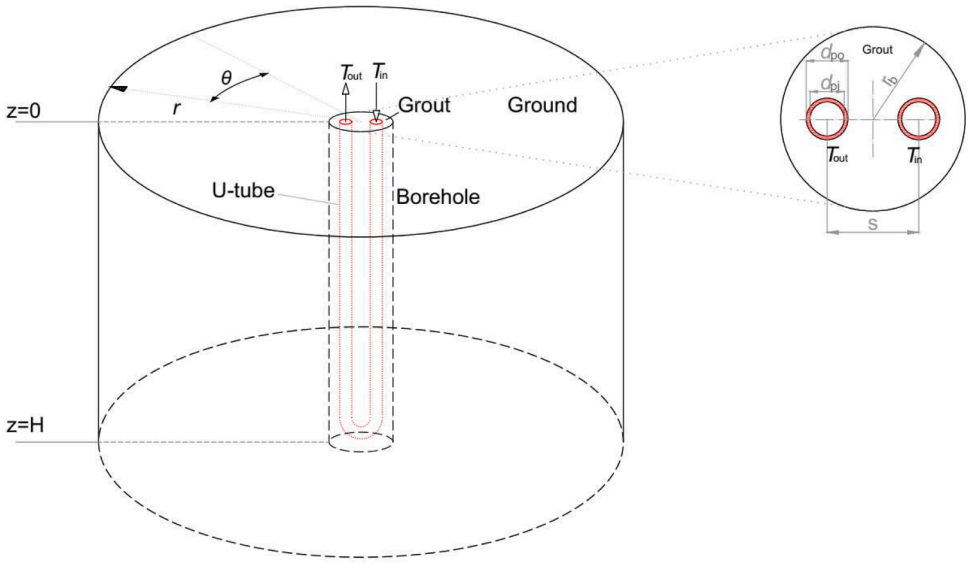

Fig. 1. Illustration of a borehole with a single U-tube.

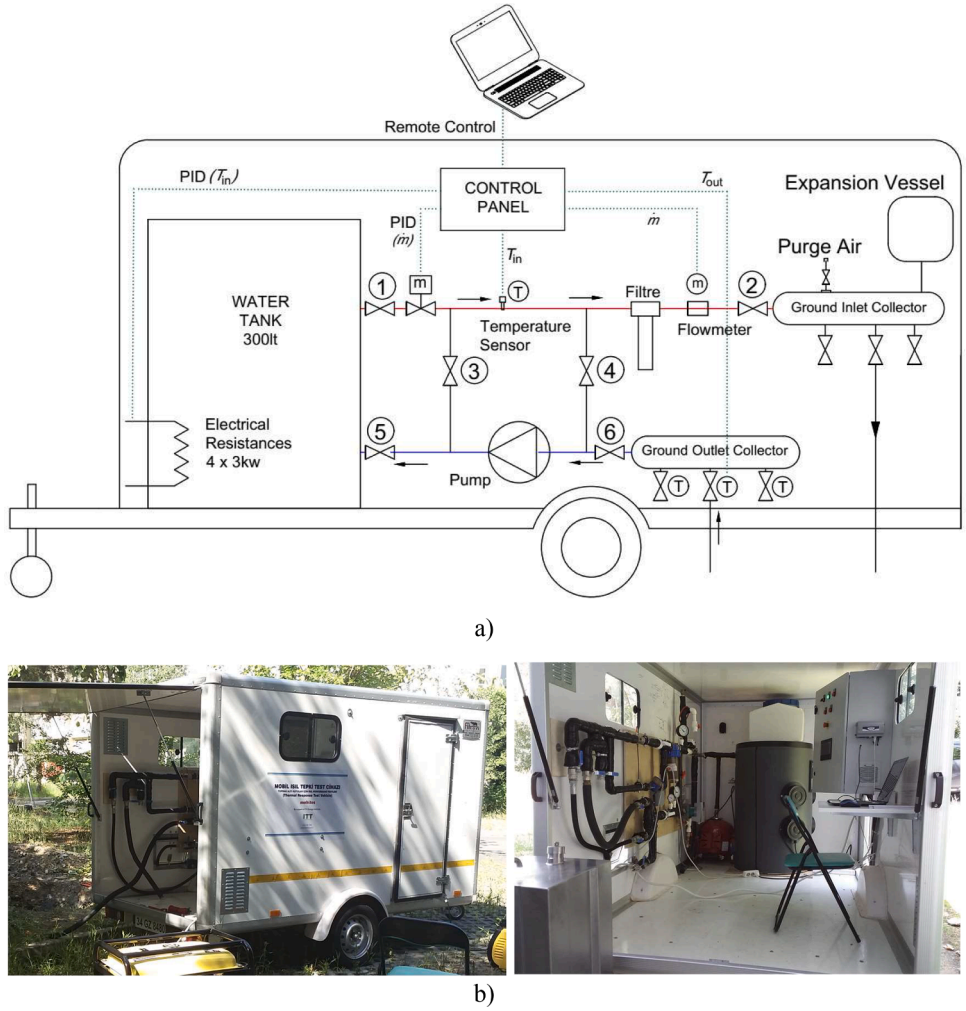

Fig. 2. A mobile flow-controlled TRT measurement unit. Flowchart (a), and exterior and interior views (b).

3. Results

Four different types of TRT approaches were performed in the same borehole. Following the recommendations of the ASHRAE (2011), sufficient waiting time is allowed between the tests. The thermal conductivity estimations are made using experimental data of different TRTs,

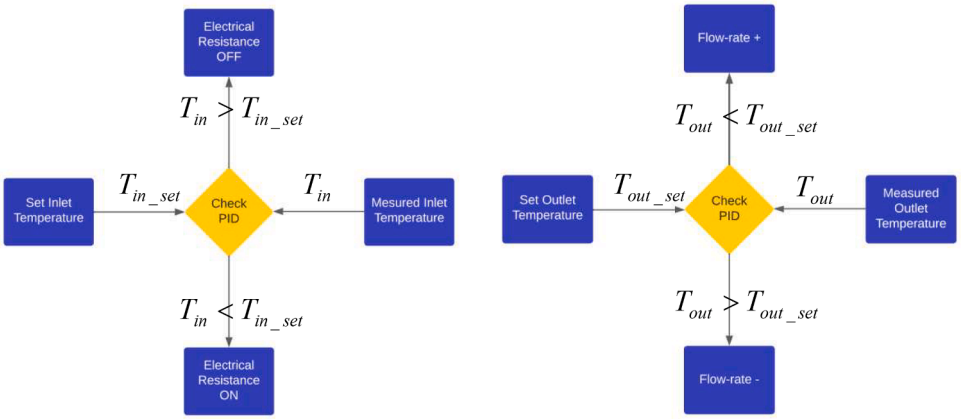

Fig. 3. Flowcharts of PID controllers for inlet and outlet temperatures.

Table 1
Properties of the borehole and ground.

Borehole depth	H	56	m
Borehole radius	r_b	0.108	m
Shank space	s	0.072	m
Pipe's outer diameter	d_{po}	0.032	m
Pipe's inner diameter	d_{pi}	0.026	m
Thermal conductivity of pipes	k_p	0.38	W/(m·K)
Thermal conductivity of grout	k_g	1.2	W/(m·K)
Ground density	ρ_g	2390	kg/m^3
Specific heat capacity of ground	c_{gr}	860	J/(kg·K)

and the results are compared.

3.1. CIT-TRT: T_{in} and $\dot{V}_f$ are constant

Fig. 4 shows the inlet and outlet fluid temperatures and the flow rate during the test. T_{in} and $\dot{V}_f$ were kept constant and T_{out} free to change. A plot of $1/q'$ versus $\ln(t)$ and the best straight-line fit through the experimental data are seen in Fig. 5. Using Eq. (2), the thermal conductivity is estimated as 1.94 W/(m·K) with the Mean Absolute Percentage Error (MAPE) of 2.6. The MAPE values are determined by $MAPE = (100/N)\sum_{j=1}^{N} q_j^{'\,\mathrm{mod}} \left|(1/q_j^{'\exp}) - (1/q_j^{'\,\mathrm{mod}})\right|$, where the superscripts "exp" and "mod" represent the values from the experiment and the model, respectively.

3.2. CHF-TRT: q' and $\dot{V}_f$ are constant

The heat flux is kept constant equal to $q' = 63$ W/m during the second test period of 47.1 h. The measured inlet and outlet temperatures and flow rate are given in Fig. 6. Fig. 7 shows the average circulated fluid temperature ($\overline{T}_{wf}$) in a logarithmic time scale. The fitting process is demonstrated in Fig. 7 and the following equation is fitted to the data (Witte, H. 2016)

$$T_f = \beta_{chf}\left[\ln(t) + \ln\left(\frac{4\alpha}{e^{\gamma}(r_b)^2}\right)\right] + q' R_b + T_\infty, \tag{4}$$

where R_b (m·K/W) and T_∞ represent borehole thermal resistance and undisturbed underground temperature respectively. Eq. (4) suggests that the thermal conductivity of the ground can be estimated from the slope of the fluid temperature β_{chf} (K) by using

$$k = \frac{q'}{4\pi\beta_{chf}}. \tag{5}$$

The red line in Fig. 7 represents the best fit obtained with the least-squares method. Obtaining the slope β_{chf} from the best fit and using it in Eq. (5), thermal conductivity is calculated as 1.73 W/(m·K). This value is lower than 1.94 W/(m·K) estimated by CIT-TRT. This difference results from the fluctuations of outlet temperature during the test, although it is assumed to be constant in the model. As mentioned in the previous section, keeping the outlet temperature constant during the test is

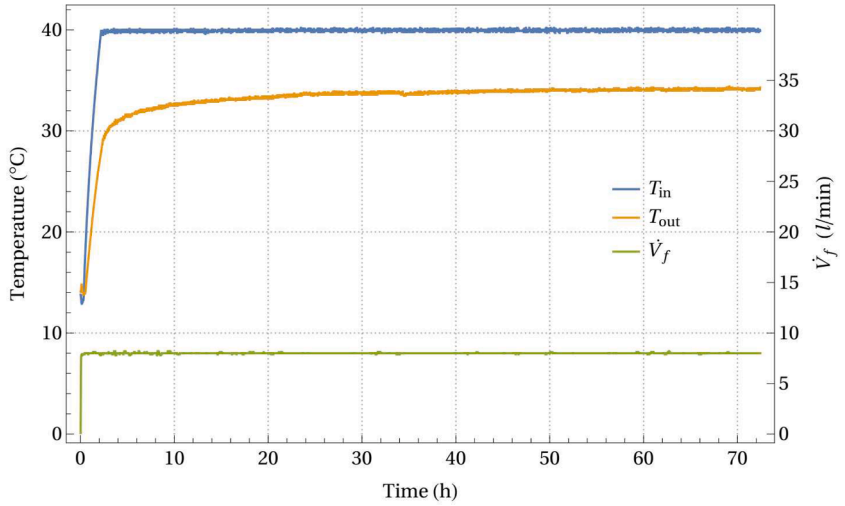

Fig. 4. Time variations of inlet and outlet fluid temperatures and flow rate during the CIT-TRT.

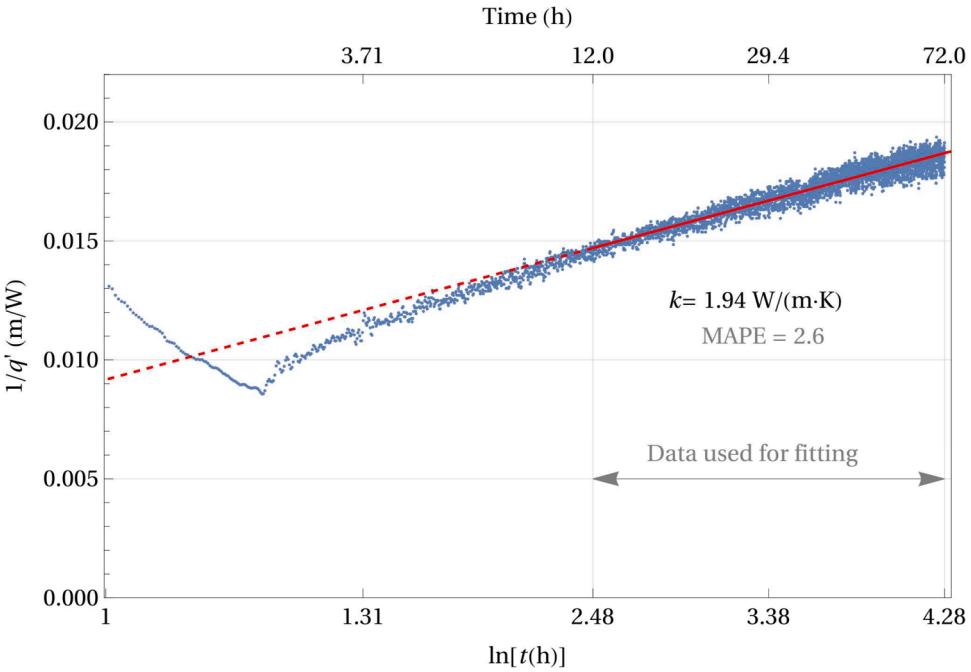

Fig. 5. Estimation of ***k***-value of the ground by using the CIT-TRT data for T_{in} =40 °C. The blue dots show the experimental data and the solid red line represents the fitted line to determine the slope value β in Eq. (2), respectively. The dashed red line shows the fitted part's extension into the early stages.

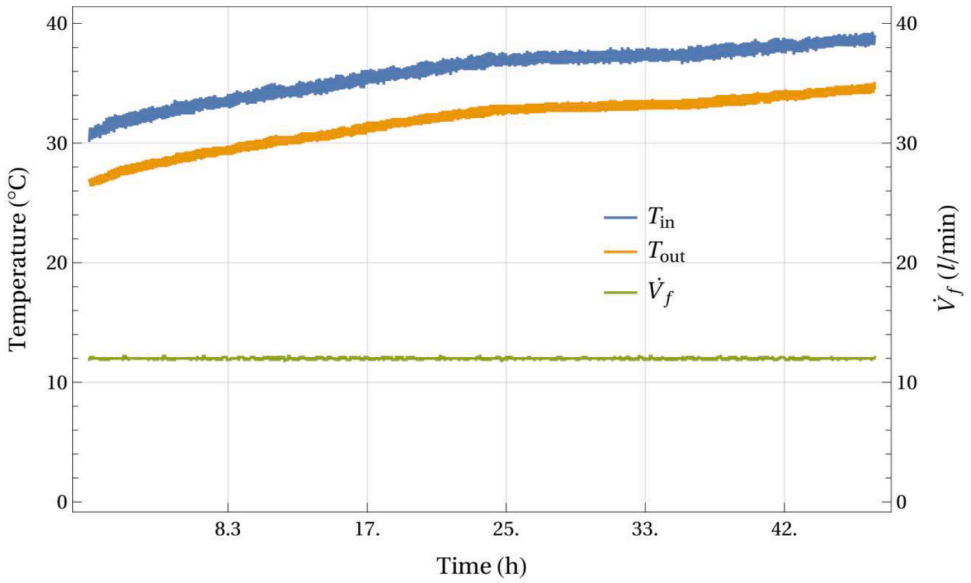

Fig. 6. Time variations of inlet and outlet fluid temperatures and flow rate during the CHF-TRT.

possible. In the following subsection, the effect of double temperature control on the results is experimentally examined.

3.3. CT-TRT: T_{in} and T_{out} are constant

Three tests with different temperature values are performed to examine the influence of temperature difference, $\Delta T_f = T_{in} - T_{out}$, on the estimated k values. For the first one, T_{in}=35 °C and T_{out}=29 °C are the set values. Fig. 8 shows the time variations of inlet and outlet temperatures besides the flow rate. It takes approximately 8 h to reach a steady-state regime for the temperatures. The flow rate takes high values to keep the T_{out} constant at this transient regime, and after 45 h, it approaches its steady value of 6 l/min.

Fig. 9 shows a plot of $1/q'$ versus $\ln(t)$. The red line shows the best-fitting range for the least-squares method. The thermal conductivity is estimated as 1.80 W/(m·K). The vertical gridlines in Fig. 9 represent the time range used in the fitting process. We use the data for the range of 11.7–60 h.

The second test was performed for T_{in}=40 °C and T_{out}=35 °C. Fig. 10 shows the time variations of T_{in}, T_{out} and $\dot{V}_f$. Steady-state condition is reached for the temperatures after 10 h. The steady value of flow rate appears after 50 h as 9 l/min. A plot of $1/q'$ versus $\ln(t)$ is seen in Fig. 11.

For the last test of this section, the chosen inlet and outlet temperatures are T_{in} =50 °C and T_{out} =43 °C. In Fig. 12, we see the time variations of T_{in}, T_{out} and $\dot{V}_f$. Similarly, after roughly 10 h, a steady-state condition is achieved for the temperatures. The steady value of flow rate appears after 100 h as 9 l/min. Fig. 13 shows the plot of $1/q'$ versus

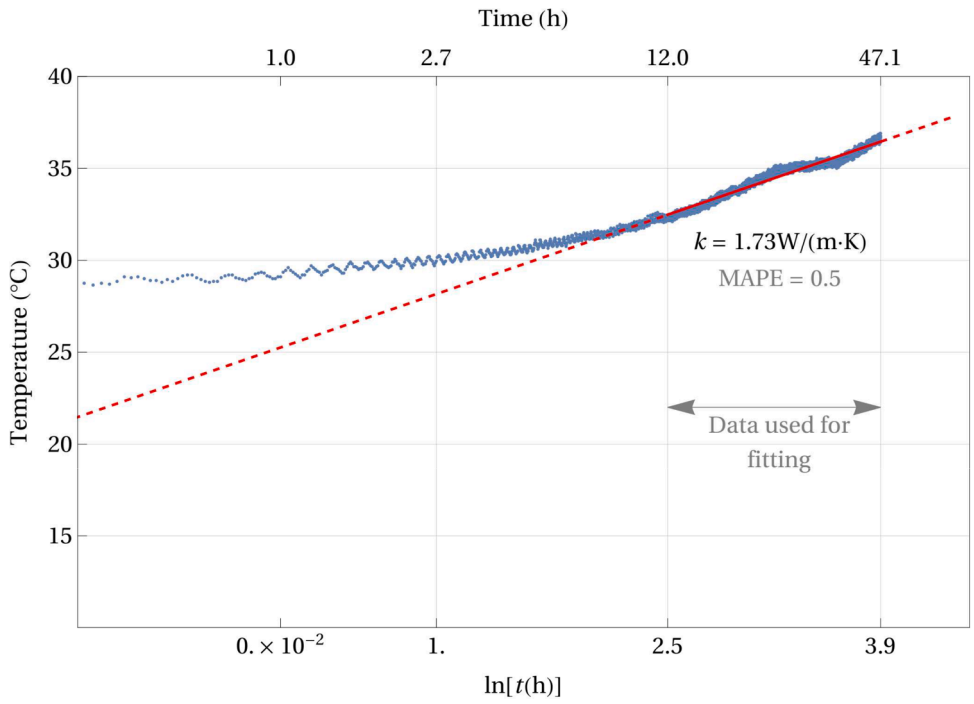

Fig. 7. Change in the average fluid temperature ($\overline{T}_{wf}$) during the experiment versus logarithmic time scale and estimation of ***k***-value of the ground by using the CHT-TRT data for $\dot{q}' = 63\,\mathrm{W/m}$. The blue dots show the experimental data and the solid red line represents the fitted line to determine the slope value β_{chf} in Eq. (5), respectively. The dashed red line shows the fitted part's extension into the early stages.

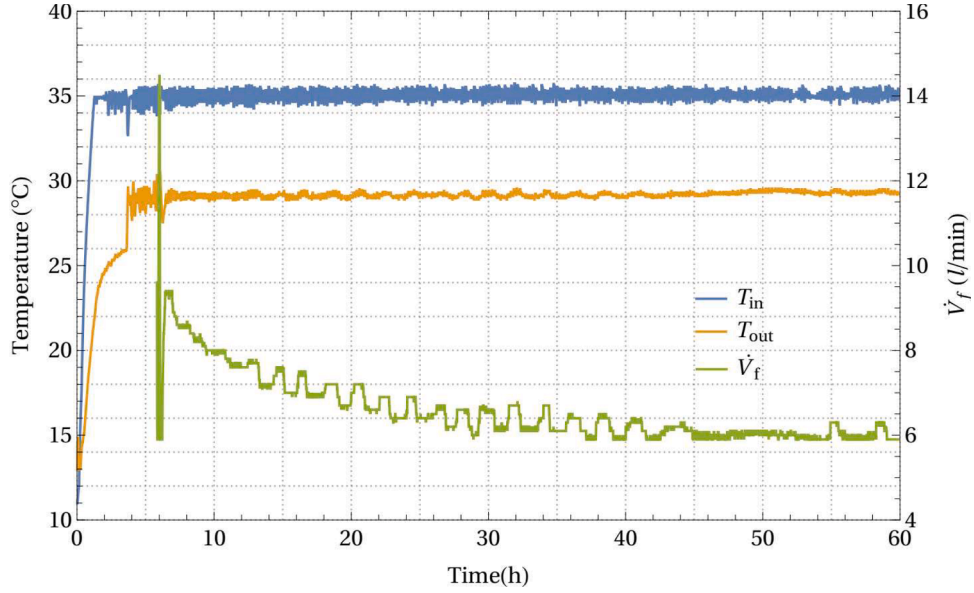

Fig. 8. Time variations of inlet and outlet fluid temperatures and flow rate during the CT-TRT, T_{in} =35 °C and T_{out} =29 °C.

ln(t).

From these three different CT-TRT data, the k-values are estimated as 1.80 W/m·K, 1.77 W/m·K, and 1.65 W/m·K for the fluid temperatures of 35–29 °C, 40–35 °C, and 50–43 °C, respectively. It shows the influence of temperature level on the estimated k-values in CT-TRT. CHF-TRT estimates 1.73 W/m·K for the k-value when the fluid temperatures are set as 40–30 °C (see Fig. 6). Therefore, as expected, the best agreement between CHF-TRT and CT-TRT is obtained for the same temperature interval, 40–35 °C, as 1.73 W/m·K and 1.77 W/m·K. In a CIT-TRT, flow rate has a considerable effect on the results and the best way is to choose the highest possible value for the flow rate to keep the temperature difference minimum. Besides that, to obtain similar results from CIT-TRT and CHF-TRT, both tests must be set for the same temperature range.

3.4. CIT&CHF-TRT: T_{in} and $\dot{q}'$ are constant

Using FC-TRT, it is also possible to perform a TRT under both constant heat flux and constant inlet temperature conditions simultaneously. Thus, as an alternative TRT, we pumped the constant temperature water, T_{in}=35 °C, into BHE and controlled the flow rate to fix the heat flux equal to $\dot{q}' = 54\,\mathrm{W/m}$. The test results are given in

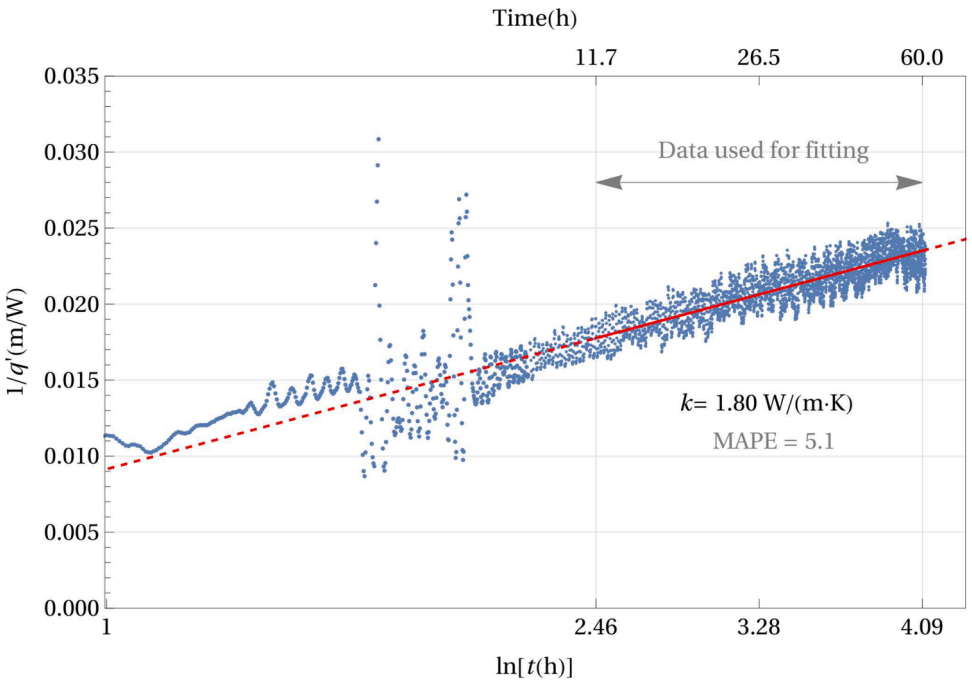

Fig. 9. Estimation of k-value of the ground by using the CT-TRT data for T_{in} =35 °C and T_{out} =29 °C. The blue dots show the experimental data and the solid red line represents the fitted line to determine the slope value β in Eq. (2), respectively. The dashed red line shows the fitted part's extension into the early stages.

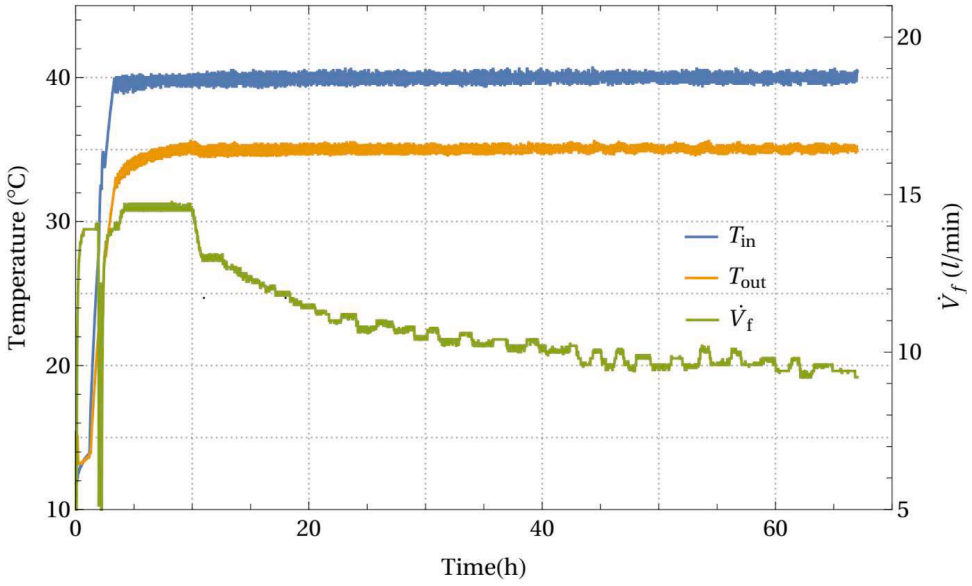

Fig. 10. Time variations of inlet and outlet fluid temperatures and flow rate during the CT-TRT for T_{in} =40 °C and T_{out} =35 °C.

Fig. 14.

The variation of the average circulated fluid temperature $\overline{T}_{wf}$ with $\ln(t)$is given in Fig. 15. Temperature fluctuations are lower than in the conventional test shown in Fig. 7 because both T_{in} and q' are kept constant. The estimated k-value is 1.61 W/m·K.

4. Uncertainty analysis

For the TRTs consisting of constant heat flux condition, Test-2 and Test-6 in Table 2, the thermal conductivity is determined from $k = \rho_f c_f V_f \Delta T_f / 4\pi\beta_{chf} H$ by using Eqs. (3) and (5). Hence, the relative uncertainty of k-value is given by Witte (2013) and calculated as

$$\frac{\delta k}{k} = \sqrt{\left(\frac{\delta \dot{V}_f}{\dot{V}_f}\right)^2 + \left(\frac{\delta \Delta T_f}{\Delta T_f}\right)^2 + \left(\frac{\delta \beta_{chf}}{\beta_{chf}}\right)^2 + \left(\frac{\delta \rho_f}{\rho_f}\right)^2 + \left(\frac{\delta c_f}{c_f}\right)^2 + \left(\frac{\delta H}{H}\right)^2} \tag{6}$$

where $\delta\dot{V}_f$ is the uncertainty of flow rate measured by a magnetic flowmeter with $\delta\dot{V}_f = 0.1$ l/min. ΔT_f represents the difference between inlet and outlet fluid temperatures, T_{in} and T_{out}, measured by A-type PT100 sensors with an uncertainty of 0.15 K. Therefore, $\delta\Delta T_f = \sqrt{(\delta T_{in})^2 + (\delta T_{out})^2}$ is determined as 0.212 K. For the maximum and minimum temperatures in Table 2, the relative uncertainty values of fluid density and heat capacity, $\delta\rho_f/\rho_f$ and $\delta c_f/c_f$, are 0.8% and 0.3%

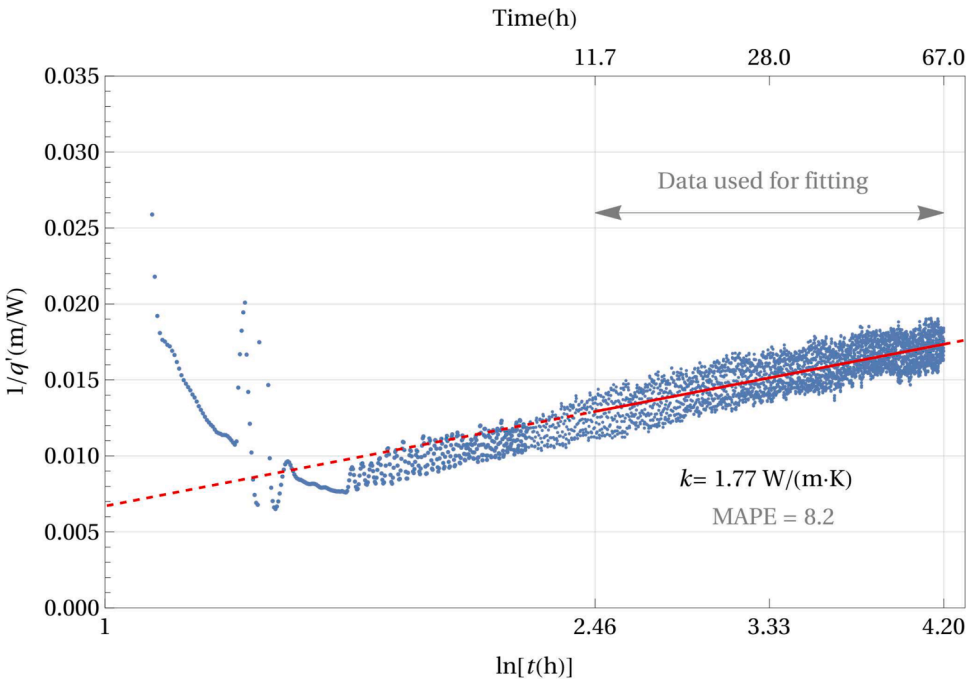

Fig. 11. Estimation of k -value of the ground by using the CT-TRT data for T_{in} =40 °C and T_{out} =35 °C. The blue dots show the experimental data, and the solid red line represents the fitted line to determine the slope value β in Eq. (2), respectively. The dashed red line shows the fitted part's extension into the early stages.

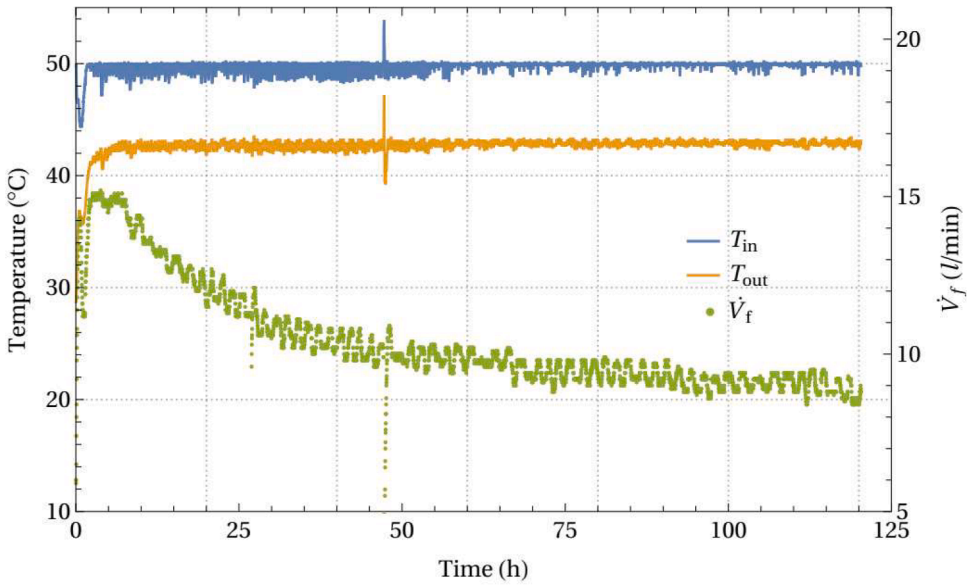

Fig. 12. Time variations of inlet and outlet fluid temperatures and flow rate during the CT-TRT for T_{in} =50 °C and T_{out} =43 °C.

respectively. Also, $\delta\beta_{chf}/\beta_{chf}$ is represented by MAPE values in Table 2. The relative uncertainty of BHE depth is considered as $\delta H/H = 1\%$, Witte (2013). By using these values, $\delta k/k$ is calculated by Eq. (6) for Tests-2 and 6 and its values are given in Table 2.

Similarly, for the TRTs consisting of constant temperature conditions, Eq. (2) is used to determine the value of k. Thus, its relative uncertainty is

$$\frac{\delta k}{k} = \sqrt{\left(\frac{\delta \Delta T}{\Delta T}\right)^2 + \left(\frac{\delta \beta}{\beta}\right)^2} \tag{7}$$

where $\delta\Delta T = \sqrt{\delta\overline{T}_{wf}^2 + \delta\overline{T}_{\infty}^2}$ and $\delta\overline{T}_{wf} = \delta\Delta T_f$. The ground temperature is measured from 5 different points and, according to Witte (2013), $\delta\overline{T}_{\infty} = \sqrt{\sum_{i=1}^{5}[\delta T_{\infty}(z_i)]^2}/5$, which gives 0.067 K. Use of the values of $\delta\overline{T}_{\infty} = 0.067$ Kand $\delta\Delta T_f = 0.212$ K gives $\delta\Delta T = 0.222$ K. Therefore, the values of $\delta k/k$ are determined by Eq. (7) and given in Table 2 for Tests-1, 3, 4 and 5. As temperatures and/or flow rates change through the tests, uncertainties also change. In Table 2, however, the maximum uncertainty values are given.

5. Discussion and conclusions

All test results are summarized in Table 2. Undisturbed ground temperatures are measured by the temperature sensors located between

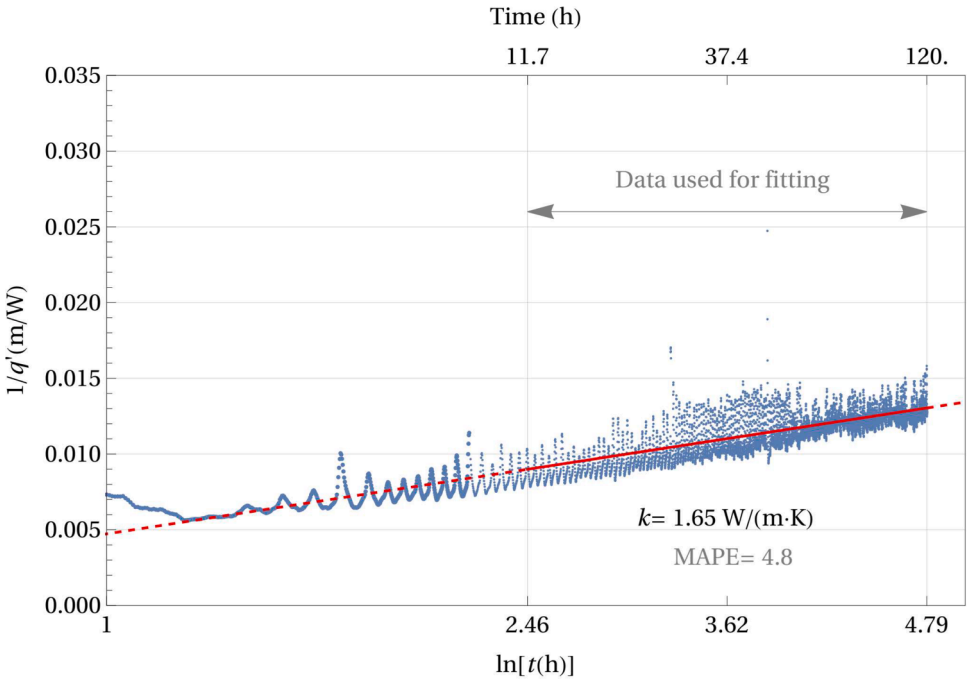

Fig. 13. Estimation of ***k***-value of the ground by using the CT-TRT data for T_{in} =50 °C and T_{out} =43 °C. The blue dots show the experimental data and the solid red line represents the fitted line to determine the slope value β in Eq. (2), respectively. The dashed red line shows the fitted part's extension into the early stages.

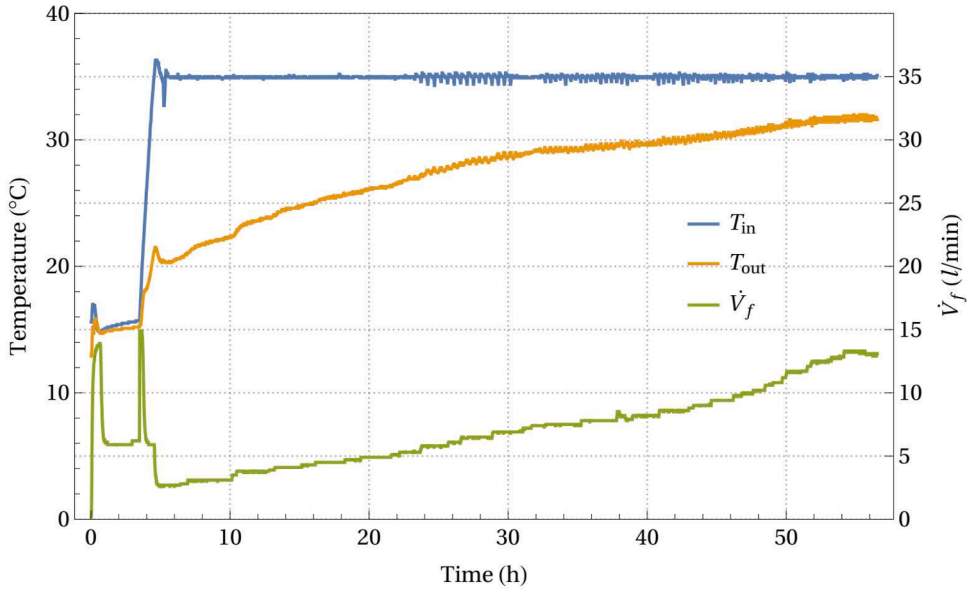

Fig. 14. Time variations of inlet and outlet fluid temperatures and flow rate during the CIT&CHF-TRT for T_{in} =35 °C and q' =54 W/m.

the U-pipe and the grout of the borehole at each 10 m depth of the borehole. The symbol "∼" represents the time-dependent quantities during TRT. CIT-TRT estimates slightly higher *k*-values than the others because of the delayed steady-state regime (20 h after the beginning) due to uncontrolled outlet temperature and the higher temperature difference, $\Delta T_f \approx 6$ °C, caused by the low flow rate chosen. On the other hand, the flow control keeps both inlet and outlet temperatures constant, and it causes better agreement between the conventional CHF-TRT and CT-TRT results. The lower the temperature difference, the better the agreement. The estimated *k*-values of CT-TRT for 40–35 °C and CHF-TRT are 1.77 and 1.73 W/(m·K), respectively. The estimation of CIT&CHF-TRT, 1.61 W/(m·K), is the smallest *k*-value but still agrees with CT-TRT estimations in the 7% maximum deviation range.

During the CT-TRT for 35.1 – 29.2 °C, the flow rate changes between 6 and 12 l/minin the first 25 h of the test, Fig. 8, although it becomes less than 10 % after the 25th hour of the test. Therefore, it is necessary to know whether the borehole thermal resistance is considerably affected due to the changes in flow rate. Using the explicit formula of the Multipole method given by Claesson and Javed (2019), the effect of the flow rate on the borehole thermal resistance can be estimated. Even for the interval of 6–12 l/min, thermal resistance changes are in a completely negligible range, from 0.199 to 0.197 m·K/W. Therefore, the total change of borehole thermal resistance is about 1 % from the beginning to the end of the test.

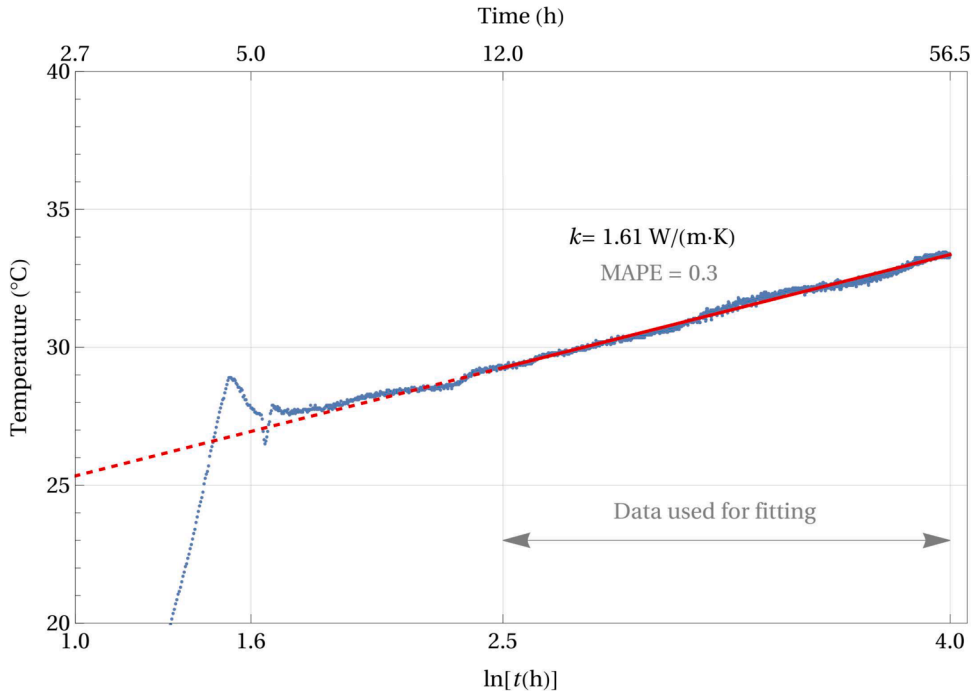

Fig. 15. Change in the average fluid temperature ($\overline{T}_{wf}$) during the experiment with logarithmic time scale and estimation of thermal conductivity (***k***) of ground by using the data of CIT&CHF-TRT. The blue dots show the experimental data, and the solid red line represents the fitted line to determine the slope value β in Eq. (5), respectively. The dashed red line shows the fitted part's extension into the early stages.

Table 2
Summary of all test results. The symbol "∼" represents the time-dependent quantities during TRT measurements. The average uncertainty in estimated k-values is approximately 5% due to measurement devices.

No	TRT	Constant quantities	T_{in} (°C)	T_{out}(°C)	$\dot{V}_f$ (l/min)	$q^{'}$ (W/m)	T_{∞} (°C)	k-value W/(m·K)	MAPE
1	CIT-TRT	T_{in}, $\dot{V}_f$	40.0	∼	8.0	∼	18.8	1.94 ± 2.9 %	2.6
2	CHF-TRT	$q^{'}$, $\dot{V}_f$	∼	∼	12.0	63.1	18.5	1.73 ± 5.3 %	0.5
3	CT-TRT	T_{in}, T_{out}	35.1	29.2	∼	∼	19.6	1.80 ± 5.4 %	5.1
4	CT-TRT	T_{in}, T_{out}	40.0	35.1	∼	∼	19.8	1.77 ± 8.3 %	8.2
5	CT-TRT	T_{in}, T_{out}	49.8	42.8	∼	∼	18.4	1.65 ± 4.9 %	4.8
6	CIT&CHF-TRT	T_{in}, $q^{'}$	35.0	∼	∼	53.6	19.2	1.61 ± 5.0 %	0.3

- In the previous study about constant temperature TRT, Aydin et al. (2019) showed that the slope of the inverse heat transfer rate in logarithmic time axes is related to only the thermal conductivity of the ground but not the heat capacity, and thus can be used for direct estimation of thermal conductivity. Naturally, the estimations based on constant temperature and constant heat flux models are expected to be the same in principle. However, the deviations from constant temperature conditions in practice affect the accuracy of the estimations and might cause some inconsistency between the estimations of CT-TRT and CHF-TRT. Note that the constant power or heat flux condition is relatively more manageable than the constant temperature condition. For a constant inlet temperature test, outlet temperature changes asymptotically through the test, as seen in Fig. 4. This is the main reason for the deviation from the conditions of the analytical model.
- On the other hand, the introduced FC-TRT keeps both inlet and outlet fluid temperatures simultaneously constant and leads to more accurate estimations for thermal conductivity. By using the introduced system, three CT-TRTs are performed at different temperatures, and their average estimation for thermal conductivity is 1.74 W/(m·K), while the conventional CH-TRT estimates 1.73 W/(m·K). Also, it is seen that the temperature level of the test is another factor affecting the estimated values. Therefore, the best agreement between CT-TRT and CHF-TRT can be achieved if their temperature ranges are the same.
- Furthermore, four different TRT methods are compared, and a good agreement is obtained between their estimations. Also, the introduced FC-TRT system provides a generalized and precise TRT platform and allows the performance of both CIT-, CT-, and CHF-TRTs besides the novel CIT&CHF-TRT. Therefore, FC-TRT offers more opportunities for researchers, planners, and engineers.

CRediT authorship contribution statement

Murat Aydin: Funding acquisition, Conceptualization, Methodology, Formal analysis, Data curation, Visualization, Writing – original draft, Writing – review & editing. **Ayse Ozdogan Dolcek:** Data curation, Investigation, Writing – review & editing. **Mustafa Onur:** Conceptualization, Methodology, Supervision, Writing – review & editing. **Altug Sisman:** Conceptualization, Methodology, Validation, Supervision, Writing – review & editing.

Declaration of competing interest

The authors declare that they have no known competing financial interests or personal relationships that could have appeared to influence the work reported in this paper.

Data availability

Data will be made available on request.

Acknowledgments

We thank the Balıkesir University Scientific Research Projects Unit for partially funding this study. We are also grateful to Prof. Dr. Sebastian Bauer for his valuable discussions, Mehmet Ertuğral for his support in the design and implementation of the test system, and Tolga Dolcek for his help in conducting experimental tests on the field.

References

ASHRAE, 2011. ASHRAE handbook: HVAC applications. Atlanta, GA, USA: 2011.
Aydin, M., Onur, M., Sisman, A., 2019. A new method for analysis of constant-temperature thermal response tests. Geothermics 78, 1–8. https://doi.org/10.1016/j.geothermics.2018.11.001.
Aydin, M., Sisman, A. and Gultekin, A., 2014. Long Term Performance Prediction of a Borehole and Determination of Optimal Thermal Response Test Duration, Proceedings of 39th Workshop on Geothermal Reservoir Engineering, Stanford University, February 24-26, 2014, Stanford/California, (USA).
Beier, R.A., Mitchell, M.S., Spitler, J.D., Javed, S., 2018. Validation of borehole heat exchanger models against multi-flow rate thermal response tests. Geothermics 71, 55–68. https://doi.org/10.1016/j.geothermics.2017.08.006.
Beier, R.A., 2021. Analysis of thermal response tests on boreholes with controlled inlet temperatures versus controlled heat input rate. Geothermics 94, 102099.
Bussmann, G., Stöckert, F., Güldenhaupt, J., Tünte, H., 2016. EGRT Und Bohrlochgeophysik an Der Neuen 500 M-Bohrung FEcampus_R1 Des GZB in Bochum. Der Geothermiekongress, Essen, 30.11.2016.
Carslaw, H.S., Jaeger, J.C., 1959. Conduction of Heat in Solids. Claremore Press, Oxford, UK (Chapter XIII).
Choi, W., Kikumoto, H., Ooka, R., 2018. New perspectives in thermal performance test: cost-effective apparatus and extended data analysis. Energy Build 180, 109–121. https://doi.org/10.1016/j.enbuild.2018.08.008.
Claesson, J., Javed, S., 2019. Explicit multipole formulas and thermal network models for calculating thermal resistance of double U-pipe borehole heat exchangers. Science and Technology for the Built Environment 25 (8), 980–992. https://doi.org/10.1080/23744731.2019.1620565.
EU energy in figures, Statistical Pocketbook, 2021. 2011/833, European Union, 2021.
Guo, F., Zhu, X., Zhang, J., Yang, X., 2020. Large-scale living laboratory of seasonal borehole thermal energy storage system for urban district heating. Appl. Energy 264, 114763.
Ingersoll, L.R., Zobel, O.J., Ingersoll, A.C., 1954. Heat Conduction with Engineering Geological and Other Applications. McGraw-Hill, New York, NY, USA, p. 325.
Mogensen, P., 1983. Fluid to duct wall heat transfer in duct system heat storages. Proc. Int. Conf. Subsurf. Heat Storage Theory Pract. Swedish Counc. Build. Res. 1983, 652–657.
Raymond, J., Lamarche, L., Malo, M., 2015. Field demonstration of a first thermal response test with a low power source. Appl. Energy 147, 30–39.
Spitler, J., Bernier, M., 2016. Vertical borehole ground heat exchanger design methods. Advances in Ground-Source Heat Pump Systems 29–61.
Spitler, J., Gehlin, S., 2019. IEA HPT Annex 52: Measuring GSHP System Long-Term Performance. European Geothermal Congress 2019, Den Haag, pp. 11–14. June.
Wang, H., Qi, C., Du, H., Gu, J., 2010. Improved method and case study of thermal response test for borehole heat exchangers of ground source heat pump system. Renew Energy 35, 727–733. https://doi.org/10.1016/j.renene.2009.08.013, 2010.
Welsch, B., Völker-Göllner, L., Schulte, D.O., Bär, K., Sass, I., Schebek, L., 2018. Environmental and economic assessment of borehole thermal energy storage in district heating systems. Appl. Energy 216, 73–90.
Witte, H.J.L., 2013. Error analysis of thermal response tests. Appl. Energy 109, 302–311.
Witte, H.J.L., 2016. In situ estimation of ground thermal properties. Advances in Ground-Source Heat Pump Systems 97–116.
Zeng, H., Diao, N., Fang, Z., 2003. Heat transfer analysis of boreholes in vertical ground heat exchangers. Int. J. Heat. Mass Transf. 46, 4467–4481.